



Peak Age of Information Optimization: CSMA Versus Aloha

Dewei Wu^(✉), Wen Zhan, Xinghua Sun, and Jiyun Qiu

Shenzhen Campus of Sun Yat-sen University, Shenzhen, China
wudw5@mail2.sysu.edu.cn, {zhanw6,sunxinghua,qiujy8}@mail.sysu.edu.cn

Abstract. In this paper, we focus on the Peak Age-of-Information (PAoI) performance in Carrier Sense Multiple Access (CSMA) networks. Specifically, by assuming that sensors are equipped with unit-size buffers and the Bernoulli update process, the PAoI expression and the optimal access probability for minimizing PAoI are derived. A comparison between the optimal PAoI in CSMA and that in Aloha is presented, identifying the age performance in CSMA could be inferior to that in Aloha if the ratio of sensing time to packet length is high. The critical threshold in terms of this ratio is characterized, which is shown as a decreasing function of traffic arrival rate. It reveals that compared to CSMA, Aloha is a better choice in scenarios with large propagation delay and light traffic, such as low earth orbit mobile-satellite communications for Internet-of-Things services.

Keywords: Age of information · CSMA · Aloha

1 Introduction

With the rapid advancement of the Internet of Things (IoT), emerging IoT applications necessitate more stringent information timeliness requirements. In domains such as environmental monitoring, vehicular networking and intelligent healthcare, swift and accurate system responses are essential for enabling effective decision-making by servers [1]. In order to characterize information timeliness in wireless networks, the concept of Age-of-Information (AoI) was initially introduced in [2], which measures the time elapsed since the generation of the most recent successfully transmitted update. How to optimize AoI performance is vital for propelling networks towards heightened productivity.

As an elegant solution for multiple sensors to access a shared channel, Carrier Sense Multiple Access (CSMA), has been widely applied such as wireless ad-hoc networks and WiFi [3]. For the existing works of optimizing throughput or delay performance of CSMA, the design of optimal parameters has long been considered a challenging issue, since CSMA has the notorious bi-stability property similar to which in Aloha [4], i.e., the network may have two distinct steady operating points.

In recent years, the AoI characterization and optimization of CSMA networks have garnered considerable attention [5–10]. The studies [5, 6] focused on characterizing the average AoI performance in vehicular network scenarios under different assumptions. The paper [7] derived the closed form expression of the average AoI of a ultra dense IoT system in the presence of noisy channels by using the stochastic hybrid systems approach. The work [8] characterized the worst AoI of wireless sensor networks, revealing the necessity of tuning the contention window size to minimize AoI via numerical results. The work [9] minimized the AoI of CSMA-based ad-hoc networks by optimizing the back-off timer, while the study [10] focused on how to tune the channel attempt probability to optimize AoI performance. Note that studies [8–10] are based on the assumption that each node is always saturated by allowing dummy packets to be sent when the buffer is empty. Although this assumption simplifies the mathematical complexity, it inadvertently lowers the network performance ceiling, as dummy packets also compete for channel resources without contributing to AoI. Thus, how to exactly characterize and optimize the information timeliness in CSMA networks remains a worthwhile and critical issue.

Another representative random access protocol, Aloha permits sensors with non-empty buffers to access the channel with a specific probability at the beginning of each time slot without channel sensing [11]. In contrast, CSMA requires each sensor to sense the channel and transmit only if the channel is detected as idle. The analysis in [12] reveals that when packet length is small, the benefits of sensing may not necessarily outweigh the costs, and CSMA’s access efficiency could be inferior to that of Aloha in terms of sum rate performance. In this paper, we are interested in the following issues: Does such a threshold exist in terms of age performance? If it exists, then how does this threshold vary with system parameters? We aim to address these open issues in CSMA networks by considering the metric termed Peak Age of Information (PAoI)¹, which is defined as the maximum AoI achieved before a packet is received.

Our contributions can be summarized as follows:

- *PAoI characterization and optimization*: By leveraging the embedded Markov chain in [4], the explicit expression of PAoI in CSMA networks is derived, based on which PAoI is further minimized by properly tuning the access probability. Our analysis demonstrates that the minimum PAoI decreases with the mini-slot length and linearly increases with the number of sources when the network size is large.
- *Random access protocol comparison*: Based on our previous work [14] on Aloha protocol, we compare CSMA and Aloha regarding the optimal PAoI. It is found that CSMA outperforms Aloha only when the mini-slot length of CSMA falls below a critical threshold. This critical threshold decreases lin-

¹ The adoption of PAoI as an age metric stems from its stationary distribution, which can be conveniently characterized through established queueing theory techniques [13]. The insights gained from this analysis can also be leveraged to incorporate different age metrics, including the mean AoI.

early with the traffic arrival rate λ when the aggregate input rate $\hat{\lambda} < 0.48$; otherwise, it remains constant at 0.44.

The remaining parts of this paper are arranged as follows. The system model and preliminary analysis of bi-stable behavior are provided in Sect. 2. In Sect. 3.3, we derive PAoI and further minimize it by optimally tuning the channel access probability of each sensor. In Sect. 4, insights regarding the PAoI performance between CSMA and Aloha networks are provided. Summarizing findings are concluded in Sect. 5.

2 System Model and Problem Formulation

Consider a CSMA network consisting of n sensors and a public server. Each sensor has a unit-sized buffer and all the sensors are synchronized and can sense the channel to determine its availability. The packet arrivals obey the Bernoulli distribution with parameter λ the newly arrived packet may be dropped out when the buffer is full. With a non-empty buffer, the sensors will access the channel with probability q if the channel is idle. The packet is successfully transmitted only if there is no other concurrent transmission [15], and the packet in the buffer will keep being served until it is successfully transmitted.

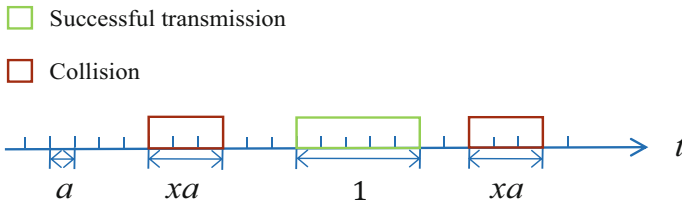


Fig. 1. Time slots in CSMA networks.

An illustration of the time slots in CSMA networks is presented in Fig. 1. Specifically, the time is divided into smaller mini-slots a , where the length a is the ratio of the propagation delay needed by each sensor for sensing the channel to the time required for packet transmission. Packets are transmitted over a noiseless channel and we assume each packet has the same size and that the transmission time required is one time slot. Suppose that the sensors can only start transmission at the start of the mini-slot, and it takes each sensor $0 \leq x \leq 1/a$ mini-slots to detect the collision and further abort the ongoing update transmission. In this paper, we assume $x = 1/a$, which indicates that the sensors are operating in the half-duplex mode and remain unaware of any collisions until the packet transmission is finished.

Let p denote the successful probability of each access. Note that a discrete-time Markov model for characterizing the Head-of-Line packets behavior in CSMA network has been established in [4]. By substituting the offered load given in Eq. (3) of [16] into the steady-state point equation given in Eq. (31) of [4], the successful transmission probability is obtained as

$$p = \exp\left(\frac{n\lambda q(1+a-p)}{\lambda(1+a-p+q)+qp}\right). \tag{1}$$

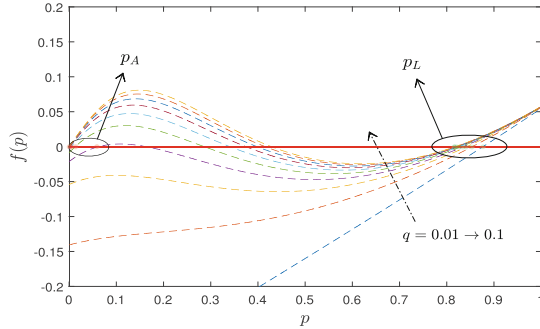


Fig. 2. Roots of (1). The intersection points of the solid line and the dashed line represent the steady-state points p_L and p_A . $n = 100$, $\lambda = 0.006$, $a = 0.1$, q is from 0.01 to 0.1 with step length 0.01.

It is clear that p is determined by the number of sensors n , the access probability q , the mini-slot length a and the traffic arrival rate λ . For illustration, we construct $f(p) = p - \exp\left(\frac{n\lambda q(1+a-p)}{\lambda(1+a-p+q)+qp}\right)$, and $f(p) = 0$ has the same roots as (1). The numerical results are presented in Fig. 2. It reveals that (1) has either one root p_L or three roots $0 < p_A < p_S < p_L < 1$, where p_A is the undesired steady-state point, p_L is the desired steady-state point and p_S is the unstable point [4]. Depending on the number of steady-state points, we can define the stable region as below:

- **Bi-stable region** $\mathcal{B} = \{(n, q, \lambda, a) \mid \text{The CSMA network has two steady-state points, } p_A \text{ and } p_L\}$.
- **Mono-stable region** $\mathcal{M} = \{(n, q, \lambda, a) \mid \text{The CSMA network has one steady-state point } p_L\}$.

The network stays either at the mono-stable region \mathcal{M} or the bi-stable region \mathcal{B} . It has long been observed that in \mathcal{B} , the network may drop from p_L to the undesired point p_A in an unpredictable way, leading to intolerable poor performance since $p_A \ll p_L$ [4]. Therefore, the network should stay in \mathcal{M} for avoiding the dropping risk. Under this consideration, our target is minimizing the PAoI

A by the optimal configuration of access probability q given the network scale n , the input rate λ and the mini-slot length a , i.e.,

$$A^* = \min_{0 < q \leq 1} A, \tag{2}$$

s. t. $\{n, q, \lambda, a\} \in \mathcal{M}$.

3 Peak Age of Information Optimization

This section aims to optimize the PAoI in CSMA networks. We will start by deriving the explicit expression of the PAoI in CSMA networks.

3.1 PAoI Analysis

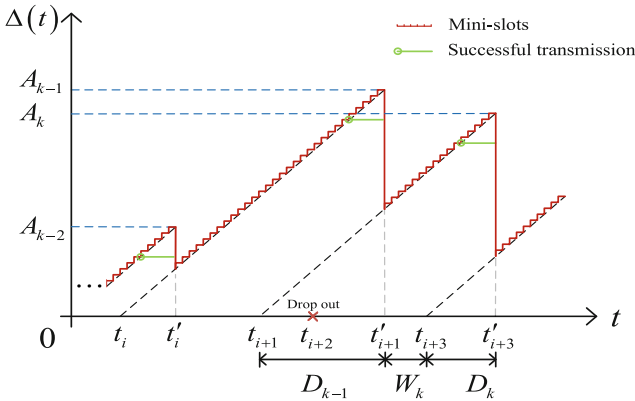


Fig. 3. AoI trace in a CSMA network with the mini-slot length $a = 0.2$.

A graphical illustration of the AoI evolution over time is presented in Fig. 3. The time instances at which each packet arrives and is successfully transmitted are denoted by t_i and t'_i respectively, $i \in \{1, 2, \dots\}$. Only successfully transmitted packets are marked in the figure. Each transmission takes 5 mini-slots, as determined by $a = 0.2$. It can be seen from Fig. 3 that the AoI $\Delta(t)$ increases over time, and $\Delta(t)$ decreases to $t - u(t)$ if and only if an update has been received by the server, where $u(t) = \max\{t_i | 0 < t'_i < t\}$ and $t \in \{1, 2, \dots\}$. Note that some packets are discarded because of the limited size of the buffer, such as the packet arrived at t_{i+2} . To avoid ambiguity, we take k to denote the index of informative packets that determine the PAoI [17, 18].

The PAoI A_k , which is defined as the AoI achieved immediately before receiving the k^{th} packet, is shown in Fig. 3. The average PAoI can be expressed as $A \triangleq \lim_{T \rightarrow \infty} \sup \frac{\sum_{t=1}^T \Delta(t) \mathbf{1}\{\Delta(t+1) \leq \Delta(t)\}}{\sum_{t=1}^T \mathbf{1}\{\Delta(t+1) \leq \Delta(t)\}}$ [19]. The informative packets are those

that arrive when the buffer is empty such as the i^{th} , $i + 1^{th}$, and $i + 3^{th}$ packets illustrated in Fig. 3. Accordingly, following the k^{th} packet reception, the PAoI A_k can be expressed as

$$A_k = D_{k-1} + W_k + D_k, \quad (3)$$

where

- D_k represents the access delay, which is the duration from the first packet to arrive after the successful transmission of the $k - 1^{th}$ packet until to the k^{th} packet. The mean access delay is given by [4]

$$E[D_k] = \frac{1}{p} + \frac{1 + a - p}{qp}. \quad (4)$$

- W_k represents the idle period, the duration from the successful transmission of $k - 1^{th}$ packet to the arrival of a new one. Note that the packet arrival rate in each mini-slot a is given by $a\lambda$, so that the idle period is obtained by

$$E[W_k] = \frac{1}{a\lambda} \cdot a = \frac{1}{\lambda}. \quad (5)$$

As W_k and D_k are independent and identically distributed random variables, we have $E[D_{k-1}] = E[D_k]$. By further combining (3)–(5), the average PAoI in CSMA networks can be expressed as

$$A = \frac{1}{\lambda} + \frac{2}{p} - \frac{2}{q} + \frac{2(1+a)}{qp}. \quad (6)$$

3.2 PAoI Optimization

The following lemma shows the optimal configuration of access probability for PAoI minimization on the condition of network state $p = p_L$.

Lemma 1. *With $p = p_L$, the optimal channel access probability for PAoI minimization is given by*

$$q_M = \begin{cases} \frac{\lambda(1+a)\left(1 + \mathbb{W}_0\left(\frac{-e^{-1}}{1+a}\right)\right)}{(1+a)\left(n\lambda + \mathbb{W}_0\left(\frac{-e^{-1}}{1+a}\right)\right) - \lambda}, & \text{if } n > \frac{\lambda(2+a-p') + p'}{\lambda(1+a)}, \\ 1, & \text{otherwise,} \end{cases} \quad (7)$$

where $\mathbb{W}_0(\cdot)$ is the principal branch of the Lambert W function and p' is the steady-state point in (1) with $q = 1$.

Proof. See Appendix A.

Lemma 1 presents the optimal access probability when the network operates at the desired steady-state point p_L . As discussed in Sect. 2, if the network stays in the bi-stable region, then it may not stay at p_L and drop to the undesired steady-state point p_A . To avoid this risk, the optimal access probability for minimizing PAoI with $\{n, q, \lambda, a\} \in \mathcal{M}$ is given by Theorem 1.

Theorem 1. For minimizing the PAoI of CSMA networks, the optimal channel access probability is given by

$$q^* = \begin{cases} \frac{\lambda(1+a)\left(1+\mathbb{W}_0\left(\frac{-e^{-1}}{1+a}\right)\right)}{(1+a)\left(n\lambda+\mathbb{W}_0\left(\frac{-e^{-1}}{1+a}\right)\right)-\lambda}, & \lambda > \lambda_0, \\ q_B, & \text{otherwise,} \end{cases} \quad (8)$$

where q_B is the non-zero root of the equation (9) and λ_0 is the non-zero root of equation $q_B = \frac{\lambda(1+a)\left(1+\mathbb{W}_0\left(\frac{-e^{-1}}{1+a}\right)\right)}{(1+a)\left(n\lambda+\mathbb{W}_0\left(\frac{-e^{-1}}{1+a}\right)\right)-\lambda}$,

$$\ln\left(\frac{n\lambda q_B^2(1+a+\lambda)}{(q_B-\lambda)^2}\left(\frac{1}{2}-\mu-\sqrt{\frac{1}{4}-\mu}\right)\right) = \frac{n\lambda q_B}{q_B-\lambda} - \frac{1}{\frac{1}{2}-\sqrt{\frac{1}{4}-\mu}}, \quad (9)$$

where $\mu = \frac{(q_B-\lambda)(1+a+q_B)}{nq_B^2(1+a+\lambda)}$.

Proof. See Appendix B.

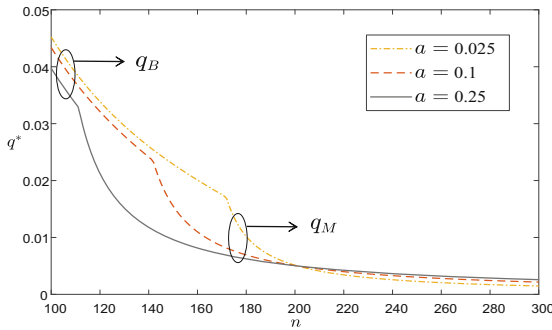


Fig. 4. Optimal channel access probability q^* versus the number of sensors n , $\lambda = 0.005$, $a = 0.025, 0.1$ or 0.25 .

By comparing Lemma 1 and Theorem 1, we see that when the packet arrival rate λ is large, the network operates at $p = p_L$ and the optimal solution is obtained according to Lemma 1. Otherwise, the network may fall into the bi-stable region \mathcal{B} and operate at $p = p_A$. In such case, Theorem 1 points out that the access probability should be set to the region boundary given by (9), with which the CSMA network can minimize PAoI while operating at $p = p_L$. Fig. 4 depicts how the optimal access probability q^* varies with the network scale with the mini-slot length $a = 0.025, 0.1$ or 0.25 . We can see that q^* decreases with the network size n . By virtue of a stronger capability of detecting channel collision, i.e., a smaller a , each sensor can take an aggressive transmission strategy with a

larger q if the network size is small. When n is large, we have $n\lambda > 1$, i.e., almost all sensors in the network have a non-empty buffer and are always listening to the channel to prepare for packet transmission. In this case, a smaller a for a certain channel idle time means more chances for making transmission decisions, therefore q^* for each mini-slot decreases slightly as a decreases to improve the successful transmission probability.

3.3 Simulation Results

Simulations are conducted to verify the above analysis. The simulation settings are identical to the system model and therefore, the details are omitted here.

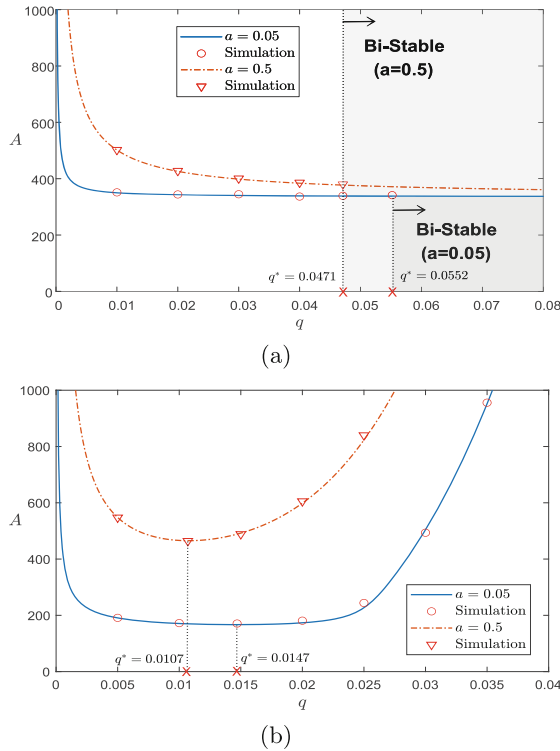


Fig. 5. PAoI A versus the channel access probability q , $n = 100$, $a = 0.05$ or 0.5 . (a) $\lambda = 0.003$. (b) $\lambda = 0.009$.

Fig. 5 illustrates how the PAoI A varies with the access probability with the mini-slot length $a \in \{0.05, 0.5\}$. The packet arrival rate is set to $\lambda = 0.003$ in Fig. 5a and $\lambda = 0.009$ in Fig. 5b. It can be observed from Fig. 5a that the PAoI A decreases as the channel access probability increase before the network falls into \mathcal{B} . However, the channel access probability should not exceed a certain

threshold to prevent the network from falling into the bi-stable region, where the network performance is unacceptable as we have discussed in Sect. 2. In addition, it can be seen that with a smaller mini-slot length a , the optimal channel access probability is higher and the corresponding minimum PAoI is also lower. A similar trend can also be observed in Fig. 5b. With $\lambda = 0.009$, the network stays in \mathcal{M} and the PAoI is minimized with $q = q^*$. The minimum PAoI can further be reduced with a smaller mini-slot length a since the source can quickly sense the channel state and make transmission decisions accordingly.

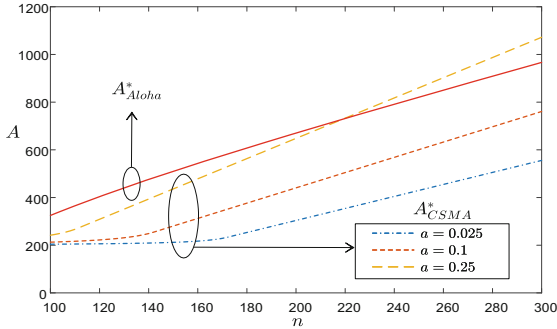


Fig. 6. Optimal PAoI A versus the number of sensors n , $q = q^*$, $\lambda = 0.005$, $a = 0.025, 0.1$ or 0.25 .

4 Minimum PAoI Comparison: CSMA Versus Aloha

So far, we have demonstrated how to tune the channel access probability for minimizing the PAoI in CSMA network. Note that another representative random access scheme, Aloha, also has drawn wide attention on age performance evaluation [20]. In contrast to CSMA, where each sensor senses the channel first and transmission happens only when the channel is idle, with Aloha, each sensor transmits if there is a request. In this section, we compare CSMA and Aloha from the view of minimum PAoI.

In our previous study [14], we evaluated and optimized PAoI of Aloha networks, where the following theorem was obtained on the optimal tuning of backoff parameters.

Theorem 2. For minimizing the PAoI of Aloha networks, the optimal channel access probability is given by

$$q_{Aloha}^* = \begin{cases} \frac{\lambda}{n\lambda - e^{-1}} & \lambda > \frac{\hat{\lambda}_0}{n}, \\ \frac{4\mathbb{W}_{-1}^2(-\frac{\sqrt{n\lambda}}{2})}{n(-2\mathbb{W}_{-1}(-\frac{\sqrt{n\lambda}}{2})-1)} & \text{otherwise,} \end{cases} \quad (10)$$

where $\hat{\lambda}_0 \approx 0.48$ and $\mathbb{W}_{-1}(\cdot)$ is the secondary branch of Lambert W function.

Proof. The proof is presented in [14].

To avoid ambiguity, let us denote the minimum PAoI of CSMA as A_{CSMA}^* and that of Aloha as A_{Aloha}^* . Fig. 6 shows how the minimum PAoI varies with n with the mini-slot length $a \in \{0.025, 0.1, 0.25\}$. It can be seen that a smaller mini-slot length a results in a lower A_{CSMA}^* . While both A_{CSMA}^* and A_{Aloha}^* increases with the network size n , especially when n is large. The use of carrier sensing has long been believed to greatly improve access efficiency. Yet, a closer look at A_{CSMA}^* with $a = 0.25$ suggests that when the network scale is large, the age performance of CSMA is inferior to that of Aloha, i.e., $A_{CSMA}^* > A_{Aloha}^*$.

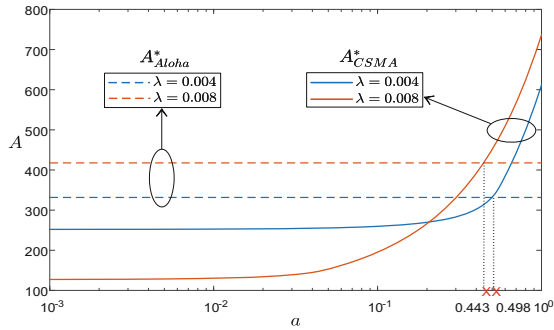


Fig. 7. PAoI A versus the mini-slot length a , $q = q^*$, $n = 100$, $\lambda = 0.004$ or 0.008 .

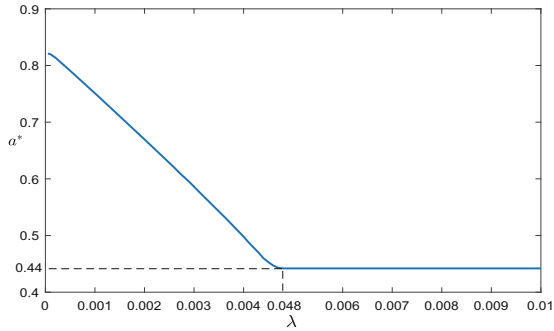


Fig. 8. Mini-slot threshold of PAoI a^* versus the packet arrival rate λ , $q = q^*$, $n = 100$.

Similar observations can also be found in Fig. 7, which illustrates how the minimum PAoI varies with the mini-slot length a and $\lambda = 0.004$ or 0.008 . The PAoI in Aloha A_{Aloha}^* remains constant since there is no carrier sensing before transmission. The PAoI in CSMA A_{CSMA}^* is lower for larger arrival rate λ when mini-slot length a is small. It is because more sources have packets to be sent instead of waiting for fresh ones passively. It is clear that with a smaller mini-slot

length a , the sensors sense the channel more frequently, which can help to avoid collision and improve the PAoI performance in CSMA networks. Yet, once more, we observe that as a increases, $A_{CSMA}^*|_{\lambda=0.004}$ outperforms $A_{CSMA}^*|_{\lambda=0.008}$ due to the negative impact of excessive channel listening overhead on network performance when a majority of sources with packets participating in contention. Furthermore, A_{CSMA}^* grows as well and finally $A_{CSMA}^* > A_{Aloha}^*$. It indicates that when the mini-slot length is large, CSMA is inferior to Aloha because the sources will experience excessive overhead in terms of channel sensing.

Let us define a critical threshold in terms of the mini-slot length a as a^* , above which $A_{CSMA}^* > A_{Aloha}^*$. Via numerical calculation according to (6) and (8) in this paper, and (10) in [14], Fig. 8 depicts how this critical threshold a^* varies with the input rate λ . It can be observed that when $\lambda > 0.048$, the critical threshold a^* is constant at 0.44 because each sensor usually has a non-empty buffer, with which the effect of λ is trivial. While, if $\lambda < 0.048$, we have $\lambda < \frac{\lambda_0}{n}$, and the optimal access probability in Theorem 2 should be adaptively tuned according to λ , with which the critical threshold a^* decreases as the input rate λ grows.

The above discussion sheds important light on practical system design. Specifically, the length of mini slots is determined by the ratio of the sensing time to the packet length, which is often limited by the propagation delay. Our analysis indicates that the benefit of sensing in CSMA is significant only for the wireless network with sufficiently small propagation delays. Yet, for non-terrestrial networks, such as low earth orbit mobile-satellite communications, where the propagation delay is expected to be large, Aloha may be a more suitable multiple access protocol than CSMA in terms of PAoI performance.

5 Conclusion

This paper presents the PAoI analysis in CSMA networks. By characterizing the steady-state points and PAoI, we derive the optimal access probability for minimizing PAoI, taking into account the bi-stability of CSMA. Furthermore, we compare the minimum PAoI in Aloha and CSMA, demonstrating that the advantage of CSMA networks is more pronounced with a smaller mini-slot length a . Specifically, there exists a critical threshold for a , where Aloha and CSMA networks exhibit the same optimal PAoI performance. Our analysis reveals that the benefit of carrier sensing for PAoI exists only when the propagation delay is small, whereas in applications with high propagation delay, such as non-terrestrial communication, Aloha may be a more suitable protocol.

It should be noted that this paper focuses on the PAoI optimization of CSMA networks based on Bernoulli packet arrival. Future work may explore optimizing PAoI with different traffic models and packet management, and explore how jointly tuning traffic rate and channel access probability to achieve better PAoI performance.

Acknowledgement. The work of W. Zhan was supported in part by The Shenzhen Science and Technology Program (No. RCBS20210706092408010), in part by National

Natural Science Foundation of China under Grant 62001524. The work of X. Sun was supported by Guangdong Basic and Applied Basic Research Foundation under Grant 2024A1515012015.

A Proof of Lemma 1

According to (1) and (6), we have

$$\frac{\partial A}{\partial q} = \frac{-2}{q^2 p^2} \left(\frac{-n\lambda^2 p q (1+a+q)\zeta^2}{(pq + \lambda(\zeta + q))^2 - n\lambda p q^2 (1+a+\lambda)} + p\zeta \right). \quad (11)$$

where $\zeta = 1 + a - p$. It can be further obtained that $\lim_{q \rightarrow 0^+} \frac{\partial A}{\partial q} < 0$. When $n > \frac{\lambda(2+a-p') + p'}{\lambda(1+a)}$, we have $\lim_{q \rightarrow 1} \frac{\partial A}{\partial q} > 0$ and the PAoI can be optimized by $q_M \in (0, 1)$, where p' is the steady-state point obtained by substituting $q = 1$ in (1) and the optimal access probability q_M can be derived by solving $\frac{\partial A}{\partial q} = 0$ that

$$q_M = \frac{\lambda(1+a-p_t)}{n\lambda(1+a) - \lambda - p_t}, \quad (12)$$

where $p_t = \exp\left(\frac{p_t}{1+a} - 1\right)$. Otherwise, we have $\frac{\partial A}{\partial q} < 0$ for $q \in (0, 1]$, and the channel access probability is given by $q = 1$. Finally, (7) is obtained by leveraging the Lambert W function and combing the above analysis.

B Proof of Theorem 1

The CSMA network region is illustrated in Fig. 9, which shares the bi-stable property in Aloha [4, 21]. It is clear that the optimal access probability q_M of (7), is included in the mono-stable region if and only if the packet arrival rate is high enough that $\lambda > \lambda_0$, where λ_0 is the intersection point of q_M and the bi-stable region boundary. Otherwise, the condition of $p = p_L$ does not hold. According to (7), we have

$$\arg \min_q A|_{\lambda > \lambda_0} = \frac{\lambda(1+a) \left(1 + \mathbb{W}_0 \left(\frac{-e^{-1}}{1+a}\right)\right)}{(1+a) \left(n\lambda + \mathbb{W}_0 \left(\frac{-e^{-1}}{1+a}\right)\right) - \lambda}. \quad (13)$$

When $\lambda < \lambda_0$, the access probability q_M will cause the network to fall into \mathcal{B} and the network performance may degenerate sharply over time [4]. Fig. 10 illustrates the PAoI in different regions, which can be observed that the PAoI with the undesired point p_A is intolerable high since the successful transmission probability $p = p_A$ is far lower than that with $p = p_L$ as Fig. 2 illustrated. The PAoI decreases with q before the network shifts to bi-stable region \mathcal{B} . In such

case, q^* is the critical value before the network falls in \mathcal{B} , which we mark as q_B and we have

$$\arg \min_q A|_{\lambda \leq \lambda_0} = q_B. \tag{14}$$

The following analysis we focus on how to solve this critical value q_B . Based on (1), let

$$f_1(p) = -\ln(p) - \frac{M}{N+p}, \tag{15}$$

where

$$M = \frac{n\lambda q^2(1+a+\lambda)}{(q-\lambda)^2}, N = \frac{\lambda(1+a+q)}{q-\lambda}. \tag{16}$$

Since $f_1(p) = 0$ is equivalent to (1), it can be utilized to analyze the number of roots. We can obtain the first derivative of $f_1(p)$ about p with respect to p as

$$f'_1(p) = \frac{g(p)}{p(N+p)^2}, \tag{17}$$

where $g(p) = -(p+N-\frac{M}{2})^2 + \frac{M^2}{4} - MN$.

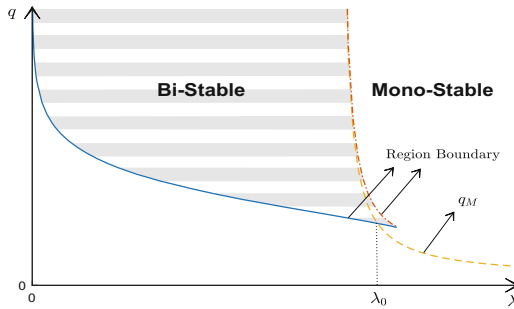


Fig. 9. The CSMA network region illustration.

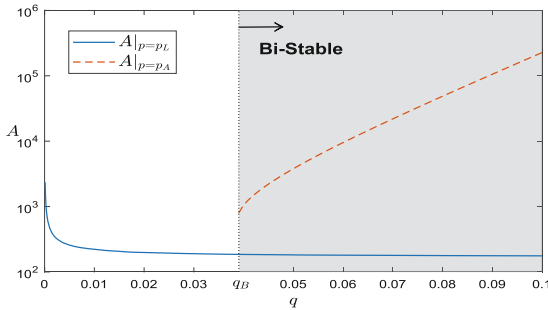


Fig. 10. PAoI performance at two distinct points p_L and p_A .

Note that $g(p)$ has the same form as Eq. (27) in [19] so we omit the root analysis in Appendix B of [19] due to the limited page. Another branch of the optimal access probability q_B , which is the boundary between the regions \mathcal{M} and \mathcal{B} , can be expressed as $f_1(p'_1) = 0$, where p'_1 is given by Eq. (29) in [19]. By combining (15), (16), q_B can be simplified as (9). Finally, the optimal channel access probability can be obtained by combining (7), (9), (13) and (14).

References

1. Guo, C., Wang, X., Liang, L., Li, G.Y.: Age of information, latency, and reliability in intelligent vehicular networks. *IEEE Net.*, Early Access. (2022). <https://doi.org/10.1109/MNET.124.2200132>
2. Kaul, S., Yates, R., Gruteser, M.: Real-time status: how often should one update? In: *Proc. IEEE INFOCOM* (2012)
3. Part 11: Wireless LAN Medium Access Control (MAC) Physics Layer 1033 (PHY) Specifications, Standard 802.11–2012 (2012)
4. Dai, L.: Toward a coherent theory of csma and aloha. *IEEE Trans. Wirel. Commun.* **12**(7), 3428–3444 (2013)
5. Kaul, S., Gruteser, M., Rai, V., Kenney, J.: Minimizing age of information in vehicular networks. In: *Proc. 8th Annu. IEEE Commun. Soc. Conf. Sensor, Mesh Ad Hoc Commun. Netw.*, pp. 350–358 (2011)
6. Baiocchi, A., Turcanu, I.: Age of information of one-hop broadcast communications in a CSMA network. *IEEE Commun. Lett.* **25**(1), 294–298 (2021)
7. Zhou, B., Saad, W.: Performance analysis of age of information in ultra-dense internet of things systems with noisy channels. *IEEE Trans. Wirel. Commun.* **21**(5), 3493–3507 (2022)
8. Moltafet, M., Leinonen, M., Codreanu, M.: Worst case age of information in wireless sensor networks: a multi-access channel. *IEEE Wirel. Commun. Lett.* **9**(3), 321–325 (2020)
9. Maatouk, A., Assaad, M., Ephremides, A.: On the age of information in a CSMA environment. *IEEE/ACM Trans. Netw.* **28**(2), 818–831 (2020)
10. Wu, Y., Wu, S., Zhang, L., Jiao, J., Zhang, N., Zhang, Q.: Random access with and without sensing in non-terrestrial networks for timely updates. In: *Proc. IEEE Int. Conf. Commun. (ICC)*, pp. 1–6 (2021)
11. Sun, X., Zhan, W., Liu, W., Li, Y., Liu, Q.: Sum rate and access delay optimization of short-packet aloha. *IEEE Open J. Commun. Soc.* **3**, 1501–1514 (2022)
12. Sun, X., Dai, L.: To sense or not to sense: a comparative study of CSMA with Aloha. *IEEE Trans. Commun.* **67**(11), 7587–7603 (2019)
13. Inoue, Y., Masuyama, H., Takine, T., Tanaka, T.: A general formula for the stationary distribution of the age of information and its application to single-server queues. *IEEE Trans. Inf. Theory* **65**(12), 8305–8324 (2019)
14. Wu, D., Zhan, W., Sun, X., Zhou, B., Liu, J.: Peak age of information optimization of slotted Aloha. In: *Proc. IEEE 96th Veh. Technol. Conf. (VTC-Fall)*, pp. 1–7 (2022)
15. Chen, X., Gatsis, K., Hassani, H., Bidokhti, S.S.: Age of information in random access channels. *IEEE Trans. Inf. Theory* **68**(10), 6548–6568 (2022)
16. Zhan, W., Dai, L.: Massive random access of machine-to-machine communications in LTE networks: modeling and throughput optimization. *IEEE Trans. Wirel. Commun.* **17**(4), 2771–2785 (2018)

17. Maatouk, A., Kriouile, S., Assaad, M., Ephremides, A.: The age of incorrect information: a new performance metric for status updates. *IEEE/ACM Trans. Netw.* **28**(5), 2215–2228 (2020)
18. Yatesp, R.D., Sun, Y., Brown, D.R., III., Kaul, S.K., Modiano, E., Ulukus, S.: Age of information: an introduction and survey. *IEEE J. Sel. Area Comm.* **39**(5), 1183–1210 (2021)
19. Sun, X., Zhao, F., Yang, H.H., Zhan, W., Wang, X., Quek, T.Q.S.: Optimizing age of information in random-access poisson networks. *IEEE Internet Things J.* **9**(9), 6816–6829 (2022)
20. Zhan, W., Wu, D., Sun, X., Guo, Z., Liu, P., Liu, J.: Peak age of information optimization of slotted aloha: FCFS versus LCFS. *IEEE Trans. Netw. Sci. Eng.*, Early Access (2023). <https://doi.org/10.1109/TNSE.2023.3272360>
21. Zhan, W., Dai, L.: Access delay optimization of M2M communications in LTE networks. *IEEE Wireless Commun. Lett.* **8**(6), 1675–1678 (2019)